

Control of Cyclin D1 and Breast Tumorigenesis by the EglN2 Prolyl Hydroxylase

Qing Zhang,^{1,7} Jinming Gu,¹ Lianjie Li,^{1,6} Jiayun Liu,¹ Biao Luo,⁴ Hiu-Wing Cheung,⁴ Jesse S. Boehm,⁴ Min Ni,¹ Christoph Geisen,¹ David E. Root,⁴ Kornelia Polyak,¹ Myles Brown,¹ Andrea L. Richardson,^{2,5} William C. Hahn,^{1,3,4} William G. Kaelin, Jr.,^{1,6,*} and Archana Bommi-Reddy^{1,7}

¹Department of Medical Oncology

²Department of Cancer Cell Biology

³Center for Genome Discovery

Dana-Farber Cancer Institute and Brigham and Women's Hospital, Harvard Medical School, Boston, MA 02115, USA

⁴Broad Institute, Cambridge, MA 02142, USA

⁵Department of Pathology, Brigham and Women's Hospital, Harvard Medical School, Boston, MA 02115, USA

⁶Howard Hughes Medical Institute, Chevy Chase, MD 20815, USA

⁷These authors contributed equally to this work

*Correspondence: william_kaelin@dfci.harvard.edu

DOI 10.1016/j.ccr.2009.09.029

SUMMARY

2-Oxoglutarate-dependent dioxygenases, including the EglN prolyl hydroxylases that regulate HIF, can be inhibited with drug-like molecules. EglN2 is estrogen inducible in breast carcinoma cells and the lone *Drosophila* EglN interacts genetically with Cyclin D1. Although EglN2 is a nonessential gene, we found that EglN2 inactivation decreases Cyclin D1 levels and suppresses mammary gland proliferation in vivo. Regulation of Cyclin D1 is a specific attribute of EglN2 among the EglN proteins and is HIF independent. Loss of EglN2 catalytic activity inhibits estrogen-dependent breast cancer tumorigenesis and can be rescued by exogenous Cyclin D1. EglN2 depletion also impairs the fitness of lung, brain, and hematopoietic cancer lines. These findings support the exploration of EglN2 inhibitors as therapeutics for estrogen-dependent breast cancer and other malignancies.

INTRODUCTION

Most successful drugs are small organic molecules that bind to, and inhibit, specific cellular proteins. Proteins that serve as enzymes have proven to be particularly tractable as drug targets. Establishing additional classes of enzymes that can be manipulated with small organic molecules opens new avenues for drug discovery.

The 2-oxoglutarate and iron-dependent dioxygenase superfamily includes the collagen prolyl and lysyl hydroxylases, the FTO and AlkB DNA demethylases, the JmjC-containing histone demethylases, the FIH1 asparaginyl hydroxylase, and the EglN family prolyl hydroxylases (Aravind and Koonin, 2001; Klose et al., 2006; Pollard et al., 2008; Taylor, 2001). These enzymes

can be inhibited with drug-like small molecules that compete with 2-oxoglutarate or interfere with iron utilization, both in vitro and in vivo (Bruegge et al., 2007; Mole et al., 2003; Ozer and Bruick, 2007; Safran et al., 2006).

There are three EglN (also called PHD or HPH) family members in humans, called EglN1, EglN2, and EglN3 (Kaelin and Ratcliffe, 2008). All three enzymes are capable of hydroxylating the α subunit of the heterodimeric transcription factor HIF (hypoxia-inducible factor). Prolyl hydroxylated HIF α is recognized by a ubiquitin ligase complex containing the pVHL tumor-suppressor protein, leading to its polyubiquitinylation and subsequent proteasomal degradation. EglN family members exhibit Km values for oxygen that exceed the oxygen concentrations found in mammalian tissues (Kaelin and Ratcliffe, 2008).

SIGNIFICANCE

Cyclin D1 plays an important role in many cancers, including breast cancer. The observations described herein predict that inhibiting EglN2 catalytic activity will diminish Cyclin D1 levels in cancer cells and impair their ability to proliferate in vivo. Notably, EglN2 is estrogen inducible and loss of either EglN2 or Cyclin D1 leads to mammary gland hypoproliferation. Therefore the relationship between EglN2 and Cyclin D1 might be especially relevant in hormone-sensitive breast cancer, in which new therapies are needed for women who become refractory to estrogen antagonists. EglN2 appears to be an attractive drug target because EglN2 is not essential in mammals and it has already been established that enzymes of this class can be inhibited with drug-like small organic molecules.

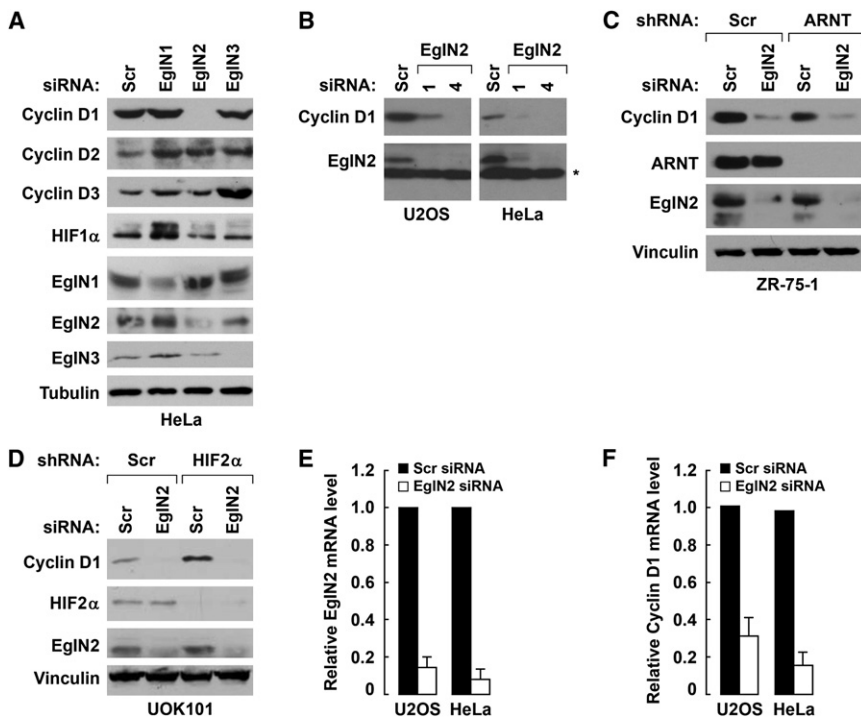


Figure 1. EglN2 Regulates Cyclin D1

(A) Immunoblot analysis of HeLa cells 48 hr after transfection with siRNAs targeting EglN1, EglN2, EglN3, or a scrambled control siRNA.

(B, E, and F) Immunoblot (B) and qRT PCR (E and F) analysis of U2OS and HeLa cells transfected with two independent siRNAs (#1 and #4) targeting EglN2 (asterisk indicates nonspecific bands). Error bars represent one SEM.

(C) Immunoblot analysis of ZR 75 1 cells infected with a lentivirus encoding an ARNT shRNA or scrambled control (Scr) followed by transfection with siRNA against EglN2 or scrambled control.

(D) Immunoblot analysis of UOK101 cells infected with a lentivirus encoding an HIF2 α shRNA or scrambled control (Scr) followed by transfection with siRNA against EglN2 or scrambled control.

Accordingly, these enzymes are highly sensitive to decrements in oxygen availability, such as might occur following an interruption in blood supply. HIF regulates a program of gene expression that facilitates survival under hypoxic conditions through cell-intrinsic changes in metabolism and cell-extrinsic changes affecting oxygen delivery. For example, HIF activates the transcription of genes such as erythropoietin that enhance red blood cell production and hence blood oxygen carrying capacity. EglN antagonists stimulate red blood cell production in mammals and are currently undergoing phase II testing for different forms of anemia (Hsieh et al., 2007; Safran et al., 2006).

EglN1 (also called PHD2) is the primary prolyl hydroxylase responsible for HIF regulation (Berra et al., 2003; Minamishima et al., 2008; Takeda et al., 2008). EglN2 (also called PHD1) and EglN3 (also called PHD3) might also regulate HIF under certain conditions (Appelhoff et al., 2004). For example, EglN3 is itself a HIF target, is induced by hypoxia, and has a lower oxygen Km than EglN1 (Appelhoff et al., 2004; Minamishima et al., 2009). Cell culture and animal experiments support that EglN3 partially compensates for EglN1 when the latter is inactivated by hypoxia (Appelhoff et al., 2004; Minamishima et al., 2009). Whether EglN2 and EglN3 have HIF-independent functions is less clear, although recent studies support a HIF-independent role for EglN3 in the control of apoptosis (Rantanen et al., 2008; Schlisio et al., 2008).

Polyak and coworkers reported that EglN2 mRNA accumulates in breast cancer cells that have been stimulated to proliferate with estrogen and that EglN2 overexpression promotes estrogen-independent growth and tamoxifen resistance (Seth et al., 2002). Frei and Edgar (2004) noted that certain phenotypes observed in flies engineered to overproduce Cyclin D1 were abrogated by concurrent inactivation of Egl9, which is the lone ancestral EglN family member in *Drosophila*. Since Cyclin D1

(2001), we asked whether EglN2 activity affects Cyclin D1 activity.

RESULTS

Toward this end, we transiently transfected HeLa cervical carcinoma cells, U2OS osteosarcoma cells, and both T47D and ZR-75-1 breast carcinoma cells with previously validated siRNAs that are specific for EglN1, EglN2, or EglN3 (Appelhoff et al., 2004). Downregulation of EglN2, but not EglN1 or EglN3, decreased Cyclin D1 protein levels (Figure 1A, Figure S1A [available online], and data not shown). Similar results were observed with a second, independent, EglN2 siRNA and downregulation of Cyclin D1 by the two different EglN2 siRNAs mirrored their ability to downregulate EglN2 (Figure 1B and Figure S1B). In some experiments Cyclin D3 was also decreased (data not shown). As expected, suppression of EglN1, but not EglN2 or EglN3, induced HIF1 α (Figure 1A). These results suggest that Cyclin D1 is specifically regulated by EglN2 among the EglN family members and that EglN2 regulates Cyclin D1 in a HIF-independent manner.

In further support of the latter conclusion, downregulation of Cyclin D1 after EglN2 loss was not affected by concurrent inactivation of the HIF α heterodimeric partner ARNT (HIF1 β) (Figure 1C and Figure S2A). In addition, EglN2 loss decreased Cyclin D1 in UOK101 and 769-P *VHL*^{-/-} renal carcinoma cells, which constitutively produce HIF2 α protein due to the absence of pVHL and produce neither HIF1 α mRNA nor protein (Maxwell et al., 1999) (Figure 1D, Figure S2B, and data not shown). Moreover, elimination of HIF2 α in these cells with a highly effective short hairpin RNA (shRNA) did not prevent the loss of Cyclin D1 in cells depleted of EglN2 (Figure 1D and Figure S2B). Collectively, these results strongly suggest that the regulation of Cyclin

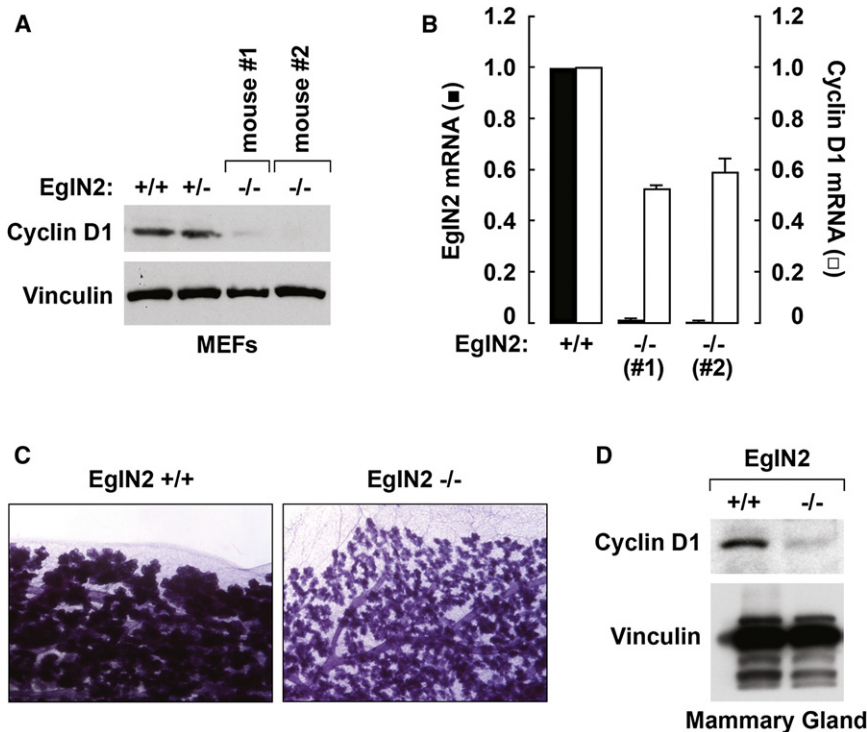


Figure 2. Decreased Cyclin D1 Levels in *Egin2*^{-/-} Mice

(A and B) Immunoblot (A) and qRT-PCR analysis (B) of MEFs prepared from littermates with the indicated genotypes. Error bars represent one SEM.

(C) Whole mounts of mammary glands from wild-type and *Egin2*^{-/-} mice 1 day postpartum. Images were taken at 6× magnification.

(D) Immunoblot analysis of mammary glands as in (C).

D1 by Egin2 is not mediated by changes in HIF activity. Note that in some experiments Egin2 protein migrated as a doublet (for example, Figure 1C), probably due to alternative translation initiation (Tian et al., 2006).

Both Egin2 mRNA and Cyclin D1 mRNA levels were diminished in cancer cells transfected with Egin2 siRNA, but not in cells transfected with a scrambled control siRNA (Figures 1E and 1F and Figures S2C and S2D). Moreover, we have not detected specific binding of Egin2 to Cyclin D1 and Egin2 failed to hydroxylate Cyclin D1 in vitro (data not shown). Collectively, these results suggest that the regulation of Cyclin D1 by Egin2 is indirect and involves changes in Cyclin D1 transcription or mRNA stability.

To examine this further, we measured the levels of heterogeneous nuclear Cyclin D1 RNA, indicative of newly transcribed mRNA precursors, and recruitment of RNA Polymerase II to the Cyclin D1 promoter, indicative of on-going transcription, in cells after Egin2 depletion. In both T47D and ZR-75-1 breast carcinoma cells depletion of Egin2 with an effective shRNA decreased heterogeneous nuclear Cyclin D1 RNA levels (Figures S3A–S3D) and decreased loading of RNA Polymerase II onto the Cyclin D1 promoter (Figures S3E and S3F) relative to cells treated with a scrambled control shRNA. In contrast, we did not detect a difference in Cyclin D1 mRNA stability in cells that were infected to produce either the Egin2 or control shRNA and then treated with actinomycin to prevent new mRNA synthesis (data not shown). Therefore the regulation of Cyclin D1 by Egin2 is at least partly at the level of transcription.

Egin2^{-/-} mice are viable and grossly normal (Aragones et al., 2008; Takeda et al., 2006). In keeping with the siRNA-based experiments described above, we found that *Cyclin D1* mRNA and protein levels are diminished in *Egin2*^{-/-} mouse embryo

fibroblasts (MEFs) (Figures 2A and 2B). Moreover, we observed that older, pregnant *Egin2*^{-/-} mice do not breastfeed their pups properly compared to littermate controls, a phenotype previously observed in *Cyclin D1*^{-/-} mice (Sicinski et al., 1995). Moreover, mammary glands from older, lactating *Egin2*^{-/-} mice revealed evidence of hypoproliferation reminiscent of, but not as severe as seen in, *Cyclin D1*^{-/-} mice (Sicinski et al., 1995) (Figure 2C) and exhibited lower levels of Cyclin D1 protein (Figure 2D). Therefore, Egin2 regulates

Cyclin D1 in vivo, with loss of Egin2 leading to a hypomorphic Cyclin D1 phenotype.

Since Egin2 mRNA is induced by estrogen in human breast cancer cells (Appelhoff et al., 2004; Seth et al., 2002), and Egin2 loss affects mammary gland proliferation, we next focused our attention on the role of Egin2 in human breast cancer. We first confirmed that Egin2 protein levels, like Egin2 mRNA levels, are induced by estrogen in human (T47D) breast cancer cells (Figures 3A and 3B). Moreover, Egin2 mRNA levels are increased in estrogen receptor (ER)-positive breast cancers compared to ER-negative breast cancers (Figures 3C and 3D) and Cyclin D1 mRNA and Egin2 mRNA levels are positively correlated with one another across breast cancers (Figure S4). In contrast, Egin1 mRNA levels appear to be highest in ER-negative, Her2-negative breast cancers and Egin3 mRNA levels highest in ER-negative, Her2-positive breast cancers (Figure 3D). Notably, both Egin1 and Egin3 are HIF targets. Although Her2 activation has been reported to activate HIF (Laughner et al., 2001; Li et al., 2005) we observed the clearest evidence of HIF activation, as determined by accumulation of canonical HIF-responsive mRNAs, in the ER-negative, Her2-negative breast cancers (A.L.R. and W.G.K., unpublished data).

Forced overexpression of Egin2 promotes colony formation by T47D cells (Seth et al., 2002). Similarly, we found that overexpression of Egin2 was sufficient to promote the proliferation of T47D cells in the absence of estrogen (Figures 3E and 3F). Exogenous Egin2 had only minimal effects on Cyclin D1 and proliferation in the presence of estrogen, however, presumably because the endogenous Egin2 is no longer limiting under these conditions (Figures 3E and 3F). To investigate whether Egin2 loss would inhibit breast cancer cell proliferation, we infected T47D cells with retroviral vectors encoding shRNAs corresponding to

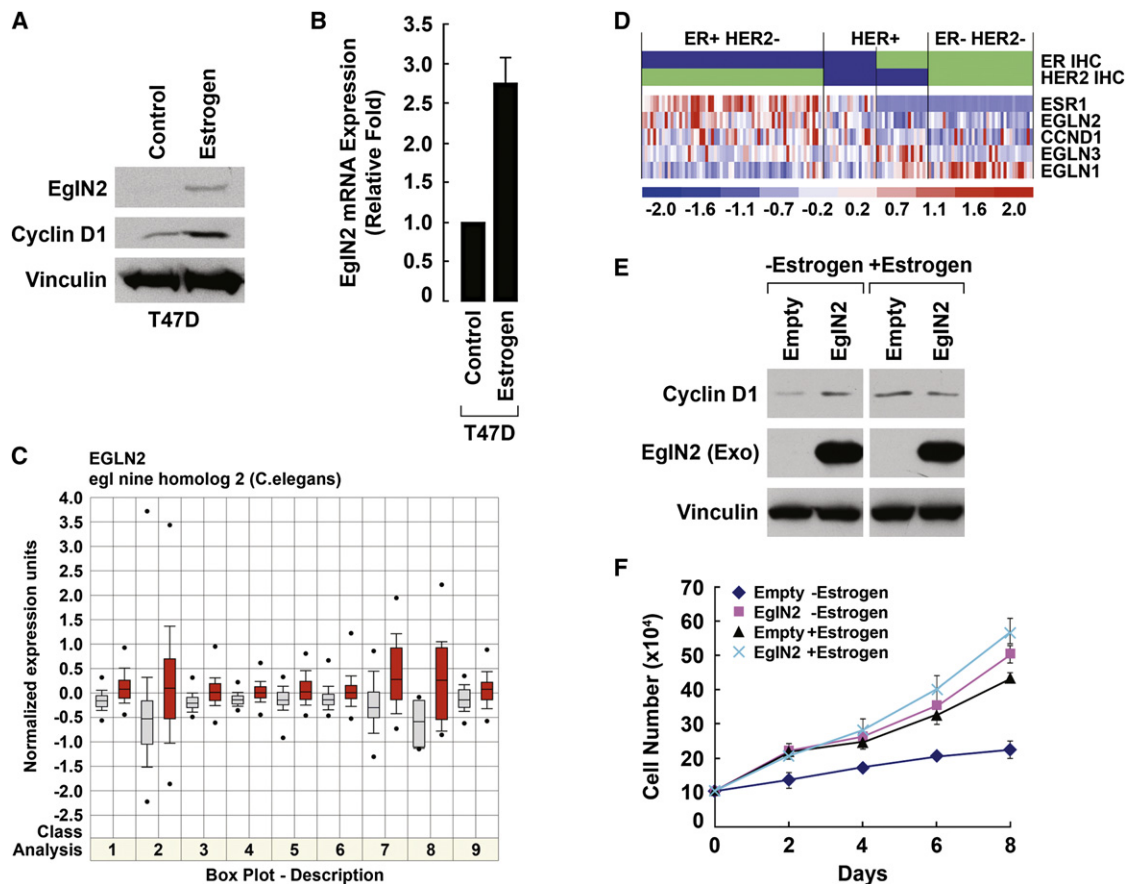


Figure 3. EglN2 Is Estrogen Inducible

(A and B) Immunoblot (A) and qRT-PCR analysis (B) of T47D cells treated with estrogen or vehicle. Error bars represent one SEM.

(C) Normalized EglN2 mRNA levels in nine publically available mRNA expression profile data sets. Red boxes, ER positive breast cancers; blue boxes, ER negative breast cancers. P values for these nine data sets are 1.2E-9; 3.4E-8; 6.2E-8; 1.1E-7; 2.1E-7; 6.3E-7; 1.4E-6; 5.6E-5; and 9.6E-5, respectively.

(D) Relative expression of EglN2 and other genes of interest in subsets of breast cancers as analyzed by gene expression array. Samples are arranged into subsets according to immunohistochemistry (IHC) staining results for ER (blue indicates $\geq 1\%$ positive nuclei and green indicates $< 1\%$ positive nuclei) and HER2/neu (blue indicates HER2/neu score of 3+ [strong complete membrane staining in $> 10\%$ of cells] and green a HER2/neu score of 0, 1, or 2+). The middle panel is a display of the relative gene expression (red indicates high expression and blue indicates low expression) with each column representing an individual tumor sample and each row representing the results for the indicated genes. Cyclin D1 (CCND1) mRNA levels are higher in ER positive tumors compared to ER negative tumors (mean levels 500 versus 330 arbitrary units; $p < 2E-8$).

(E and F) Immunoblot analysis (E) and proliferation assay (F) of T47D cells infected with retrovirus encoding HA-EglN2 or with the empty vector in the presence or absence of estrogen (10 nM) treatment. In (E), estrogen exposure was for 48 hr prior to cell harvest and anti-HA antibody was used to detect exogenous (Exo) EglN2. Error bars represent one SEM.

the two EglN2 siRNAs used above. Downregulation of both EglN2 and Cyclin D1 by the EglN2 shRNAs, but not control (scrambled GFP) shRNA, was confirmed by immunoblot analysis (Figure 4A).

As expected, T47D cells infected with the control shRNA, like parental T47D cells, proliferated in the presence of estrogen but not in its absence (Figure 4B). Proliferation in the presence of estrogen was markedly reduced, however, in T47D cells infected with either of the two EglN2 shRNAs (Figure 4B). The effects of EglN2 reduction on proliferation were even more striking in the estrogen-dependent cell lines BT-474 (Figures 4C and 4D) and ZR75-1 (Figures 4E and 4F).

The observation that two independent EglN2 shRNAs, but not the control shRNA, inhibited cell proliferation argues that this phenotype is due to effects on EglN2 activity ("on-target"). To

test this further, we performed rescue experiments using T47D cells that were infected with a retrovirus encoding a nonnatural EglN2 mRNA in which translationally silent mutations were introduced into the sequence targeted by shRNA #4. These cells, but not cells infected with an empty retrovirus, were now insensitive to the Cyclin D1 suppressive (Figure 5A) and antiproliferative effects of the EglN2 shRNA #4 (Figure 5B). These findings, together with our analysis of *EglN2*^{-/-} cells, support that EglN2 regulates Cyclin D1-dependent cell proliferation.

In parallel, we tested cells producing a shRNA #4-resistant EglN2 mRNA encoding a hydroxylase-defective EglN2 mutant (EglN2 H358A) (Epstein et al., 2001; Figure S5). This mutant, in which a canonical histidine residue within the EglN2 catalytic domain has been replaced by alanine, did not rescue cyclin D1 levels (Figure 5A) and did not rescue proliferation in T47D cells

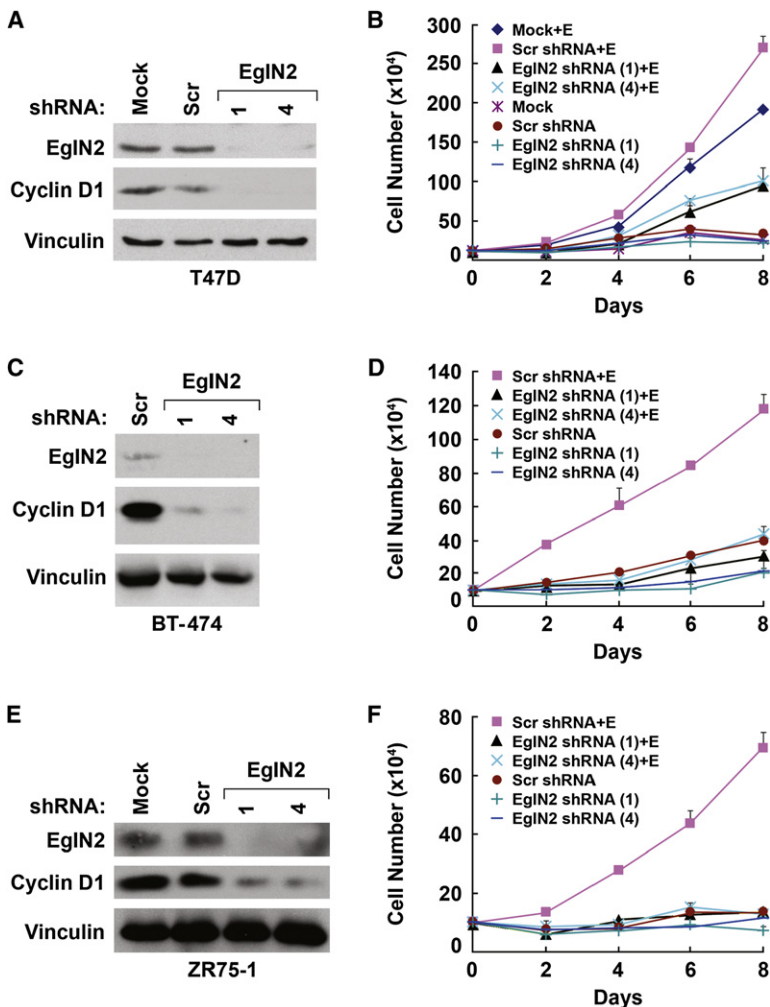


Figure 4. Downregulation of EglIN2 Suppresses Cancer Cell Proliferation

(A and B) Immunoblot (A) and cell proliferation assay (B) of T47D cells infected with retrovirus encoding shRNA against EglIN2 (sequence 1 or 4) or a scrambled control shRNA. In (B), cells were grown in Phenol red free RPMI medium supplemented with 5% charcoal/dextran treated FBS in the presence or absence of estrogen (10 nM) as indicated.

(C–F) Immunoblot (C and E) and cell proliferation (D and F) assay of BT474 (C and D) and ZR75-1 cells (E and F). Error bars represent one SEM.

infected to produce EglIN2 shRNA #4 (Figure 5B). Similarly, the retrovirus encoding wild-type EglIN2, but not EglIN2 H358A, restored Cyclin D1 in *EglIN2*^{-/-} MEFs (Figure 5C). It should be noted that the EglIN2 H358A has a shorter half-life than wild-type EglIN2 (Figure S6 and data not shown). Therefore, a higher titer of the EglIN2 H358A virus was used to achieve comparable levels of wild-type and mutant EglIN2 in Figures 5A and 5C. In viral titration experiments wild-type EglIN2 rescued Cyclin D1 levels over a wide range of titers, whereas mutant EglIN2 did not rescue at any titer tested (Figure S6 and data not shown).

Similarly, wild-type EglIN2, but not EglIN2 H358A, rescued Cyclin D1 production in HeLa cells transiently transfected with EglIN2 siRNA #4 (Figure 5D). This effect was specific because neither EglIN1 nor EglIN3 rescued Cyclin D1 levels when tested in parallel (Figure 5D). In these experiments, EglIN3, however, appeared to be unstable, possibly due to polyubiquitinylation by SIAH (Nakayama et al., 2004). Finally, endogenous Cyclin D1 levels were decreased in cells exposed to either hypoxia or small molecule hydroxylase inhibitors (Figures 5E and 5F). Downregulation of Cyclin D1 by hypoxia and hydroxylase inhibitors was due, at least in part, to decreased Cyclin D1 mRNA levels and was not an indirect consequence of activating the HIF transcriptional response as it did not depend on the canonical HIF α

partner ARNT (HIF1 β) (Figure 5F and Figure S7). These results strongly suggest that regulation of Cyclin D1 by EglIN2 is linked to the ability of EglIN2 to hydroxylate one or more substrates other than HIF.

Cyclin D1 stimulates proliferation by promoting the phosphorylation of the retinoblastoma protein (pRB) and cells lacking pRB are inured to inhibitors of Cyclin D1-associated kinase activity. Overexpression of Cyclin D1, like overexpression of EglIN2 itself, rescued cell proliferation in T47D cells expressing an EglIN2 shRNA (Figures 6A and 6B). Moreover, the proliferation of breast cancer cells lacking pRB function due to *RB1* mutation (Figures 6C and 6D), exogenous expression of the E7 oncoprotein (Figures 6E and 6F), or exogenous expression of RB1 shRNAs (Figure S8) was not impaired by EglIN2 loss despite diminished Cyclin D1 levels. These results support that impaired proliferation in cells lacking EglIN2 is due, at least partly, to loss of Cyclin D1. We also noted that exogenous Cyclin D levels were diminished by EglIN2 in some experiments (Figure 6A). The significance of this finding

is not yet clear but could reflect a posttranscriptional link between EglIN2 and Cyclin D1.

To determine whether EglIN2 ablation would diminish cancer cell proliferation or survival in other cell lineages, we obtained multiple shRNA constructs targeting EglIN2 from the RNAi Consortium (TRC) at the Broad Institute. We confirmed that each of these constructs effectively suppressed EglIN2 (Figure 7A). We next examined data from a set of 12 cancer cell lines that were screened with a pooled version of the TRC shRNA library (Luo et al., 2008) to determine whether cells harboring these EglIN2-specific shRNAs were depleted from a population of cells during 28 days. Indeed, we observed that cells expressing EglIN2-specific shRNAs were depleted from the population for each of the cell lines tested. Specifically, we observed that these constructs were depleted 2.8-fold on average with a maximum depletion of 18.4-fold for construct #5 in the U251 cell line (Figure 7B). EglIN2 ranks in the top 16.5% (rank #1553/9423 genes) of depleted genes across all 12 cell lines as compared to all genes examined in this pooled screen (Figure 7C). Together, these observations support that EglIN2 is essential for proliferation of cancer cell lines derived from multiple lineages.

To investigate whether downregulation of EglIN2 would affect tumor growth in vivo, we next infected ZR75-1 breast carcinoma

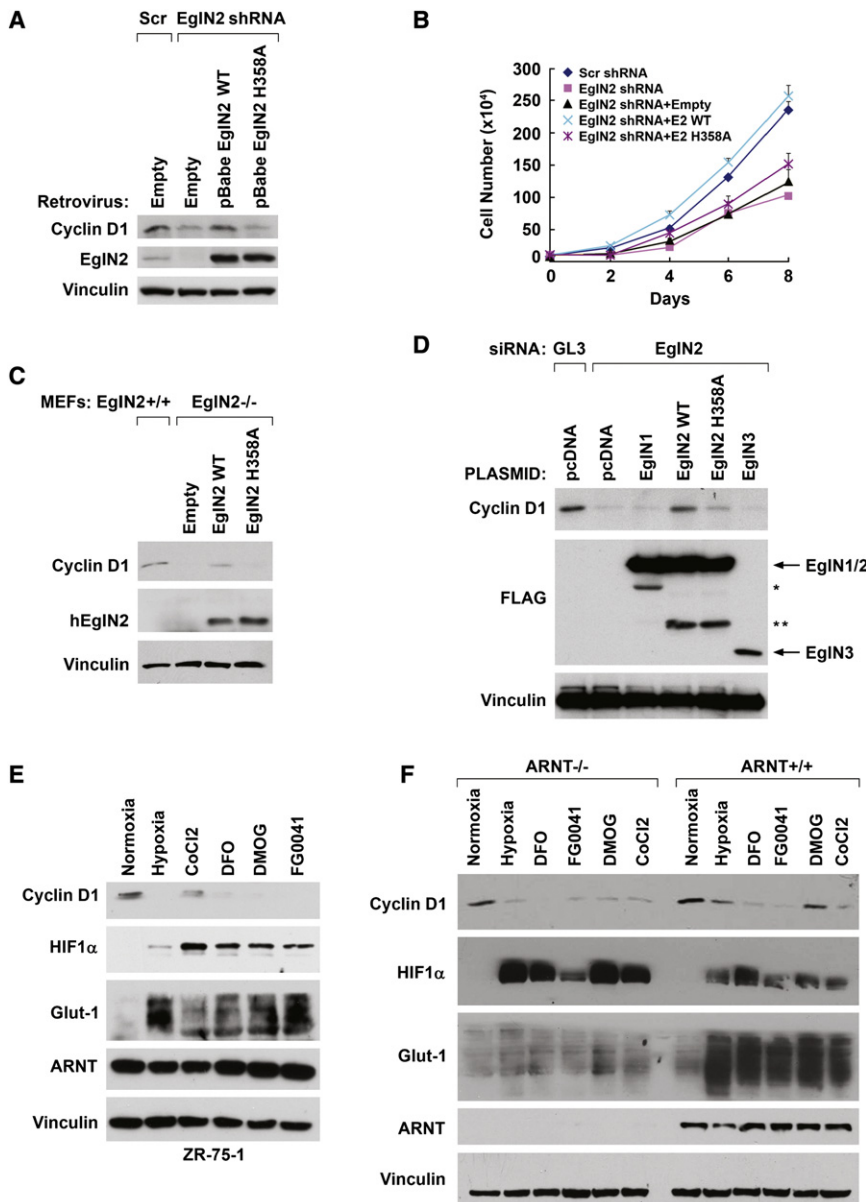


Figure 5. Control of Cyclin D1 and Proliferation by Egin2 Is Hydroxylase Dependent

(A and B) Immunoblot (A) and cell proliferation assay (B) of T47D cells that were first infected with a retrovirus expressing an shRNA resistant mRNA encoding wild type or catalytic dead (H358) Egin2 (or with empty vector) and then infected with a Egin2 shRNA retrovirus (or scrambled shRNA vector).

(C) Immunoblot analysis of Egin2^{-/-} MEFs infected with retroviruses encoding Egin2 (wild type) or Egin2 H358A or with the empty vector. An Egin2^{+/+} extract was included in lane 1 as a control. Note that the Egin2 antibody does not recognize murine Egin2.

(D) Immunoblot analysis of HeLa cells transiently transfected with plasmids encoding the indicated Egin proteins (or the empty vector) and siRNAs against Egin2 or luciferase (GL3). The molecular bases for the bands indicated by the asterisks are unknown.

(E and F) Immunoblot analysis of ZR 75 1 cell (E) and isogenic murine hepatoma cells (ARNT^{-/-} or ARNT^{+/+}) (F) treated overnight with hypoxia (0.2% O₂), CoCl₂ (200 μ M), DFO (200 μ M), DMOG (1 mM) or FG0041 (40 μ M). Error bars represent one SEM.

cells with lentiviruses encoding Egin2 shRNAs (#1 or #4) under the control of a doxycycline-inducible promoter. Cells infected with an analogous lentivirus encoding a scrambled GFP shRNA served as a control. As expected, doxycycline treatment of cells infected with the Egin2 shRNA lentiviruses led to decreased Egin2 and Cyclin D1 protein levels and decreased cell proliferation compared to cells grown in the absence of doxycycline (Figures 8A and 8B). Cessation of proliferation in this model was associated with an apparent G1/S block, consistent with loss of Cyclin D1 function (Figure S9). These effects of doxycycline were specific because they were not observed in cells infected with the control shRNA lentivirus. Gene expression profiling, combined with gene set enrichment analysis, confirmed that Egin2 depletion led to downregulation genes

linked to cell-cycle progression, estrogen-dependent signaling, and tamoxifen resistance (Figure S10 and Tables S1–S3). Next, the ZR75-1 cells infected with the inducible shRNA lentiviruses were infected with a retrovirus encoding luciferase and grown orthotopically in the mammary glands of immunocompromised mice. The luciferase activity of the Egin2 shRNA cells was comparable to the luciferase activity of the control shRNA cells in vitro (data not shown). One mammary gland was injected with the inducible Egin2 shRNA cells and the contralateral mammary gland was injected with the inducible control shRNA. Mice were treated with a depot form of estrogen to promote the growth of the breast cancer cells and live tumor cell burden was monitored noninvasively with bioluminescent imaging beginning 1 week after cell implantation. At this time point, the Egin2 shRNA tumors usually exhibited stronger luciferase signals than the control shRNA cells, arguing that the Egin2 shRNA cells were at least as tumorigenic as the control cells in vivo prior to the administration of doxycycline. Three days later, imaging was repeated. Mice in which both tumors had increased in signal intensity, indicative of tumor cell expansion, were then fed chow containing doxycycline and serially monitored using bioluminescence. Over time there was a progressive decline in the Egin2 shRNA tumor signal relative to the control shRNA tumor signal, largely due to continued expansion of the tumors formed by the control shRNA cells and an apparent arrest

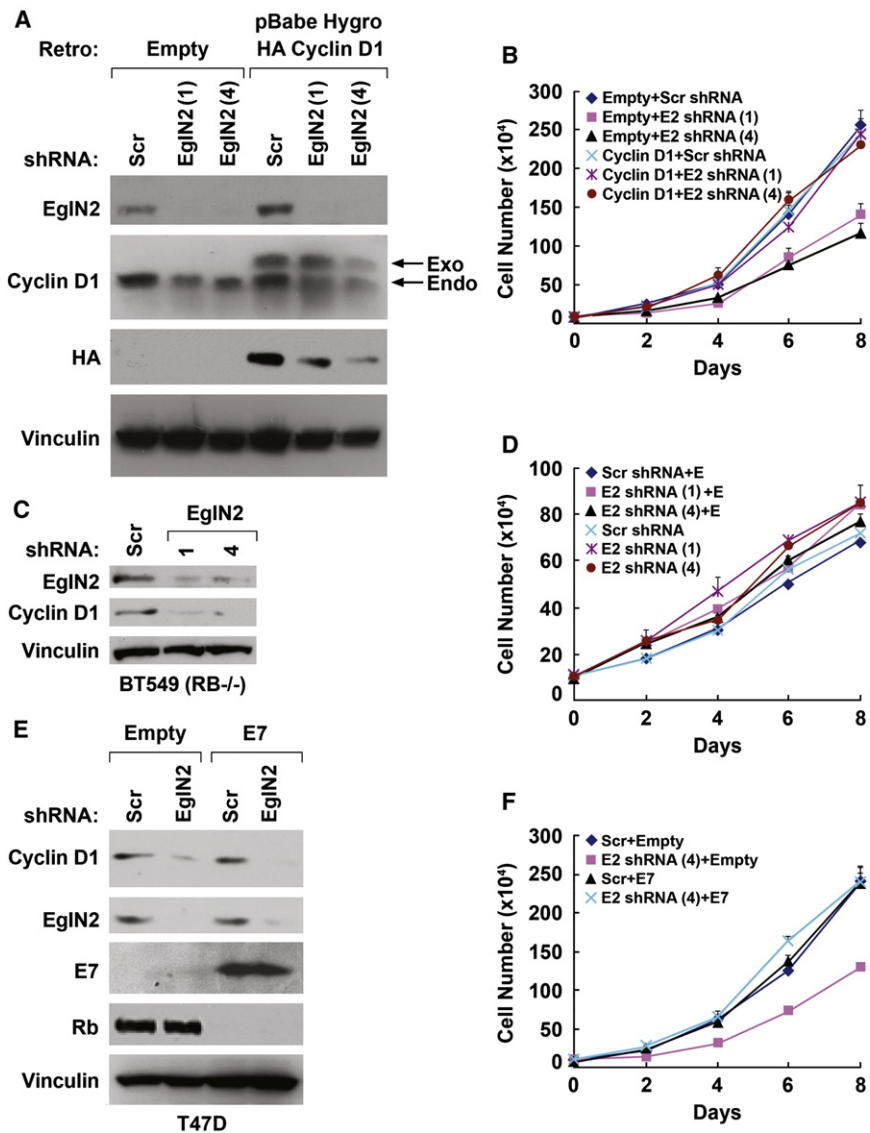


Figure 6. Impaired Proliferation of Cells Lacking Egin2 Is Due to Cyclin D1 Loss

(A and B) Immunoblot (A) and cell proliferation (B) assay of T47D cells that were infected with retroviruses encoding shRNAs against Egin2 (sequence 1 or 4) (or scrambled control) and then infected with a retrovirus encoding HA Cyclin D1 (or empty vector).

(C and D) Immunoblot (C) and cell proliferation assay (D) of BT549 RB^{-/-} breast carcinoma cells infected with retroviruses encoding shRNAs against Egin2 (sequence 1 or 4) or scrambled control shRNA. In (D) cells were grown in Phenol red free RPMI medium supplemented with 5% charcoal/dextran treated FBS in the presence or absence of estrogen (10 nM) as indicated.

(E and F) Immunoblot (E) and cell proliferation (F) assay of T47D cells that were infected with a retrovirus encoding E7 (or empty retrovirus) and then superinfected retroviruses encoding shRNAs against Egin2 (sequence 4) (or scrambled control). Note that E7 promotes the degradation of pRB (Boyer et al., 1996) and that hyperphosphorylated and hypophosphorylated pRB are not resolved under these electrophoretic conditions. Error bars represent one SEM.

DISCUSSION

We found that loss of Egin2, but not loss of the paralogous proteins Egin1 and Egin3, decreases Cyclin D1 mRNA and protein levels, decreases cell proliferation, and decreases tumor formation. Impaired proliferation in cells lacking Egin2 could be rescued by restoring Cyclin D1 protein production and was not observed in cells lacking the pRB tumor-suppressor protein, which is required for growth inhibition in cells deprived of Cyclin D1-associated kinase activity. Therefore, loss of Cyclin D1

causes, and does not merely correlate with, impaired proliferation in Egin2-defective cells. An intimate, causal connection between Egin2, Cyclin D1, and cell proliferation is also suggested by similarities between *Egin2*^{-/-} mice and *Cyclin D1*^{-/-} mice, both of which display impaired mammary gland proliferation in response to pregnancy. Regulation of Cyclin D1 and cell proliferation by Egin2 depends on Egin2 catalytic activity, suggesting that small molecule Egin2 inhibitors would have anticancer activity. Such inhibitors, were they to be developed, might be particularly useful for the treatment of estrogen-dependent breast cancer. Polyak and coworkers reported previously that Egin2 is estrogen inducible and that Egin2 overexpression promotes breast cancer cell proliferation (Seth et al., 2002). The latter observation, together with our Egin2 loss-of-function studies, indicates that Egin2 activity regulates breast cancer proliferation in response to estrogen. Cyclin D1, which is also induced by estrogen, is an important regulator of breast cancer proliferation

of the Egin2 shRNA cells (Figures 8C and 8D). After 5–6 weeks of doxycycline treatment the mice were sacrificed and the tumors were excised and weighed. Consistent with the bioluminescent images, the tumors formed by the Egin2 shRNA cells were smaller than the tumors formed by the control shRNA cells (Figures 8E and 8F). It should be noted that bioluminescent imaging detects viable tumor cells, whereas tumor mass includes contributions from stroma, host cells, and nonviable tumor cells. Similar results were observed with T47D cells (Figure S11) and MCF7 cells (Figure S12). Immunoblot analysis of ZR75-1 tumor extracts prepared at necropsy confirmed that Cyclin D1 levels were diminished in tumors after induction of the Egin2 shRNAs in vivo (Figure 8G and data not shown). Conversely, expression of Cyclin D1 under the control of a constitutively active promoter restored the ability of Egin2-depleted ZR75-1 cells to proliferate in vivo (Figure S13). Therefore, loss of Egin2 decreases Cyclin D1 levels and inhibits tumor growth in vivo.

Such inhibitors, were they to be developed, might be particularly useful for the treatment of estrogen-dependent breast cancer. Polyak and coworkers reported previously that Egin2 is estrogen inducible and that Egin2 overexpression promotes breast cancer cell proliferation (Seth et al., 2002). The latter observation, together with our Egin2 loss-of-function studies, indicates that Egin2 activity regulates breast cancer proliferation in response to estrogen. Cyclin D1, which is also induced by estrogen, is an important regulator of breast cancer proliferation

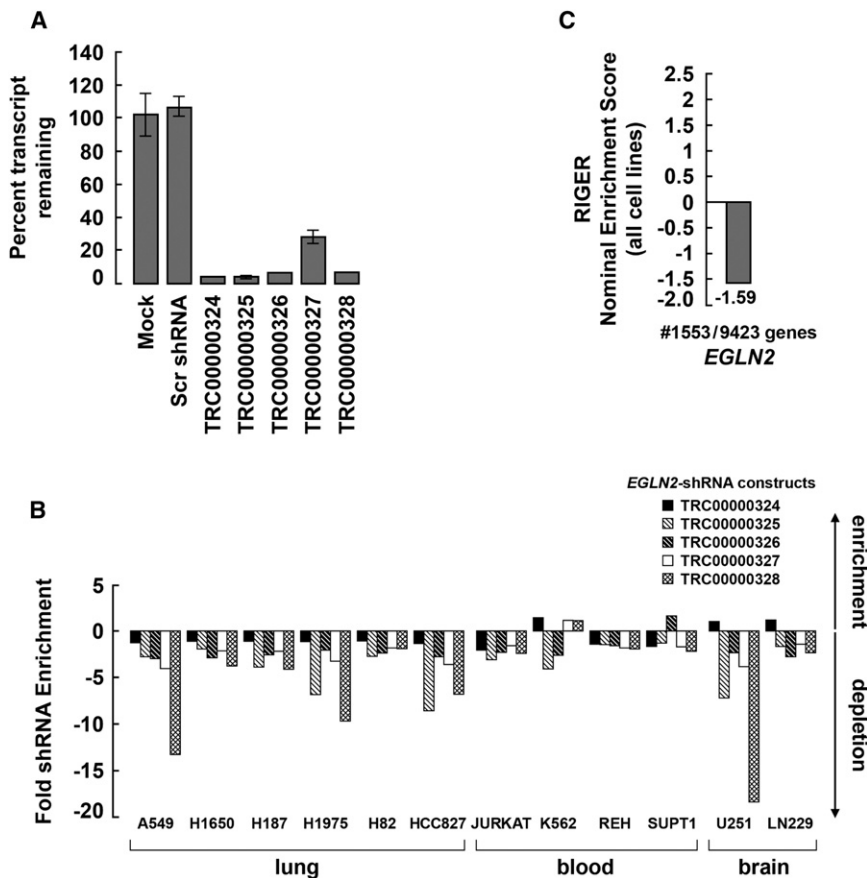


Figure 7. Impaired Fitness of Diverse Cancer Cell Lines Lacking EglN2

(A) EglN2 mRNA abundance, as determined by real time PCR, in U2OS cells infected with the indicated lentiviruses.

(B) Normalized abundance of the indicated EglN2 shRNA vectors, determined using microarray hybridization of genomic DNA, 28 days after initial infection with a pool containing ~45,000 lentiviral shRNA vectors and subsequent passage in vitro.

(C) EglN2 is an essential gene as determined by the RIGER algorithm (Luo et al., 2008). The five shRNA constructs targeting EglN2 were treated as a set that was compared to the sets derived from shRNA constructs targeting each of the other ~9,500 genes within each of the 12 cell lines shown in (B). A Kolmogorov Smirnov statistic was used for assessing bias of the *EglN2* shRNA set as showing evidence of depletion during the experiment in (B). A second application of RIGER was then used for identifying genes commonly essential among the 12 cell lines. The score and rank of *EglN2* from this analysis are shown. Error bars represent one SEM.

lacking ARNT (HIF1 β), the heterodimeric partner for HIF α , and in cells lacking pVHL, which targets hydroxylated HIF α for destruction. These observations strongly suggest that loss of Cyclin D1 upon EglN2 inactivation is not a secondary consequence of changes in HIF activity. Nonetheless, there is the potential for

and is frequently amplified or otherwise overexpressed in this disease (Roy and Thompson, 2006; Steeg and Zhou, 1998). Loss of Cyclin D1-associated kinase activity is sufficient to prevent or delay the development of breast cancer in mouse models (Landis et al., 2006; Yu et al., 2001, 2006). Cyclin D1 also has kinase-independent functions related to ER signaling and mammary epithelial proliferation (Landis et al., 2006; Neuman et al., 1997; Yu et al., 2006; Zwijnen et al., 1997). Therefore, EglN2 inhibitors might prove more efficacious than small molecule inhibitors of cdk4 and cdk6, which are the catalytic partners of Cyclin D1. Moreover, we have observed loss of the ER in breast cancer cells deprived of EglN2 (Table S2; Q.Z. and W.G.K., unpublished data). Therefore EglN2 antagonists and ER antagonists might be additive or synergistic when used to treat ER-positive breast cancers.

Downregulation of Cyclin D1 and impaired proliferation after EglN2 loss was not restricted to breast cancer cells, however, but appears to be common across a variety of tumor types. Therefore, EglN2 inhibitors might be useful beyond the treatment of ER-positive breast cancer. It will also be of interest to see if EglN2, which maps to chromosome 19q13.2, is mutationally activated in any human cancers.

Downregulation of EglN1, the primary HIF prolyl hydroxylase, led to increased HIF α , as expected, but did not decrease Cyclin D1 levels. Conversely, downregulation of EglN2 decreased Cyclin D1 without appreciably affecting HIF α protein levels. Moreover, downregulation of EglN2 decreased Cyclin D1 in cells

crosstalk between HIF and Cyclin D1. For example, HIF can transcriptionally activate REDD1, which inhibits mTOR activity (Brugarolas et al., 2004; Reiling and Hafen, 2004) and thereby decreases Cyclin D1 translation. Moreover, our findings do not in any way preclude a role for EglN2 in the regulation of HIF activity, such as has been inferred from studies of EglN2 null animals subjected to regional ischemia (Aragones et al., 2008).

Hypoxia generally inhibits cell proliferation associated with a loss of cyclin D1 and pRB hypophosphorylation presumably as a means to conserve ATP. Our findings suggest that cessation of proliferation under these conditions is due, at least partly, to impaired EglN2 activity. EglN inhibitors that are capable of activating the HIF transcriptional program in vivo are currently being tested in the clinic for the treatment of anemia and ischemic diseases. A theoretical concern with such agents relates to the ability of HIF to promote tumor growth in some preclinical models (Semenza, 2003). Our findings suggest that such protumorigenic effects might be mitigated by antitumor effects stemming from downregulation of Cyclin D1.

Clearly it will be important to determine the EglN2 substrate that links EglN2 to Cyclin D1. It should be noted that EglN2 is a nuclear protein (Metzen et al., 2003) and regulation of Cyclin D1 appears to be largely at the level of Cyclin D1 transcription. The latter was unexpected because the study by Frei and Edgar (2004) linking Egl9 to Cyclin D1 used a transgenic *Drosophila* overexpressing Cyclin D1 under the control of a heterologous promoter. It is possible that EglN2 also influences Cyclin D1

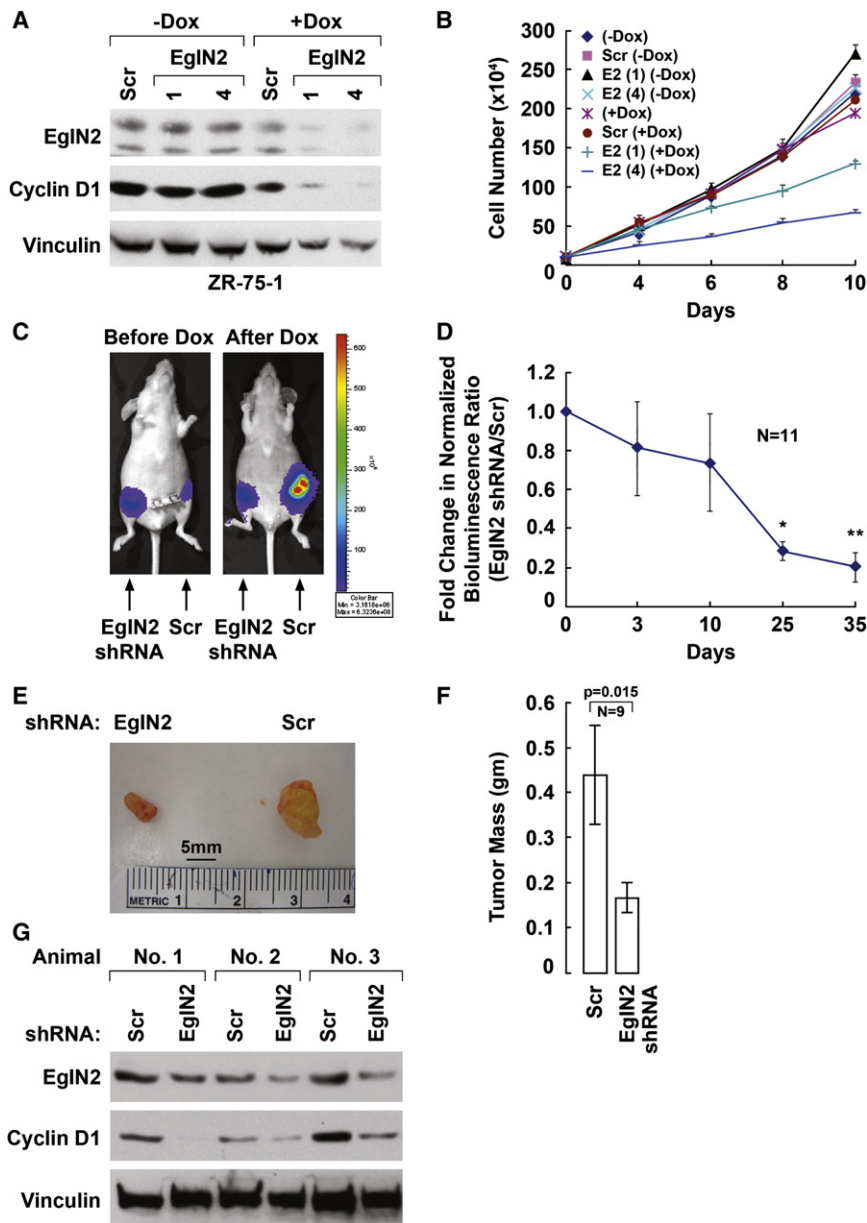


Figure 8. Downregulation of EglN2 Suppresses Tumorigenesis

(A and B) Immunoblot (A) and cell proliferation assay (B) of ZR75 1 cells infected with doxycycline (DOX) inducible lentiviruses encoding shRNAs against EglN2 (sequence 1 or 4) (or scrambled control). Cells were grown in RPMI supplemented with 10% FBS in the presence or absence of doxycycline.

(C) Representative bioluminescent images of orthotopic tumors formed by ZR75 1 cells as in (A) that were then superinfected with a retrovirus encoding firefly luciferase. A total of 8×10^6 cells were injected into the fourth mammary glands of nude mice implanted with estrogen pellets. Bioluminescent images were obtained 1 week later (day 0) and serially after mice were begun on chow containing doxycycline (day 3). Shown in (C) are the day 0 image (Before Dox) and day 35 image (After Dox). (D) Quantitation of imaging studies as in (C). * $p < 0.01$ for comparison between day 25 and day 0; ** $p < 0.01$ for comparison between day 35 and day 0. Error bars represent one SEM. See Experimental Procedures for normalization.

(E) Representative gross appearance of tumors at necropsy.

(F) Mean tumor weight at necropsy. Error bars represent one SEM.

(G) Immunoblot analysis of tumors removed from three mice at necropsy.

10 μ g/ml insulin. 769 P, ZR 75 1, BT 474, T47D, and BT 549 cells were maintained in RPMI medium containing 10% FBS except where indicated. Following retroviral or lentiviral infection, cells were maintained in the presence of hygromycin (200 μ g/ml) or puromycin (2 μ g/ml) depending on the vector. All cells were maintained at 37°C in 10% CO₂.

Mice

EglN2^{-/-} mice were obtained from Regeneron Pharmaceuticals. Inguinal mammary glands were removed one day postpartum and whole mounts were prepared as described previously (Geng et al., 1999). MEFs were isolated from embryonic day 13.5 embryos as described previously (Kozar et al., 2004).

All mouse experiments complied with National Institutes of Health guidelines and were approved by the Dana Farber Cancer Institute Animal Care and Use Committee.

siRNA

Cells grown in 6 well plates were transfected with 200 nM siRNA with Lipofect amine2000 (for mixtures of plasmids and siRNA oligos) or Oligofectamine (for siRNA alone). siRNAs were purchased from Dharmacon, Inc. Sense strands were as follows: GFP, 5' GGCTACGTCCAGGAGCGCACC 3'; GL3, 5' CTAC GCTGAGTACTTCGATT 3'; GFP Scramble, 5' AACAGTCGCGTTTGCGACTG G 3'; EglN2 A, 5' GACTATATCGTGCCCTGCATG 3'; EglN2 4, 5' GCCACTC TTTGACCGGTTGCT 3'; EGLN1, 5' AGCTCCTCTACTGCTGCA 3'; EGLN3, 5' CAGGTTATGTTCCGACGT 3' (Appelhoff et al., 2004; Schlisio et al., 2008).

Immunoblot Analysis

Whole cell extracts were prepared in EBC buffer (50 mM Tris [pH 8.0], 120 mM NaCl, and 0.5% NP40) containing protease inhibitors. Mouse mammary glands were lysed in NP 40 lysis buffer (10% glycerol, 50 mM Tris HCl

posttranscriptionally or that the findings of Frei and Edgar (2004) were unrelated to the EglN2 biology described here and therefore fortuitous. Regardless, higher metazoans, in contrast to *Drosophila* and *Caenorhabditis*, have three EglN family members. Our findings, together with previously published work, indicate that EglN1 has been retained as the primary HIF regulator under normal conditions and that EglN2 and EglN3, in addition to regulating HIF, have assumed HIF-independent roles in the control of proliferation and apoptosis, respectively.

EXPERIMENTAL PROCEDURES

Cell Culture

HeLa, U2OS, MEFs, UOK101, Phoenix, 293T, MCF7, ARNT^{-/-}, and ARNT^{+/-} cells were maintained in DMEM containing 10% fetal bovine serum (FBS) (Hyclone) except where indicated. The MCF7 media was supplemented with

[pH 7.5], 150 mM NaCl, 1% NP 40, 1 mM phenylmethylsulfonyl fluoride, and 2 $\mu\text{g/ml}$ leupeptin and aprotinin). Equal amounts of protein, as determined by the Bradford assay, were resolved by SDS PAGE and western blot analysis was performed as previously described (Schlisio et al., 2008). Rabbit polyclonal anti EglN1, EglN2, EglN3, HIF1 α , and Glut1 antibodies were from Novus Biological. Anti Cyclin D1, D2, and D3 antibodies were from Neomarker. ARNT antibody was from BD Biosciences. Anti HA antibody was from Covance. Antibodies against Vinculin, Tubulin, and FLAG (M2) were from Sigma.

Real-Time RT-PCR

Total RNA was isolated with RNeasy mini kit with on column DNase digestion (QIAGEN). First strand cDNA was generated with the StrataScript First Stand Synthesis System (Stratagene). Real time PCR was performed in duplicate with QuantiTect SYBR Green PCR master mix (QIAGEN) and the Mx3000P QPCR system (Stratagene). All values were normalized to the level of 18S rRNA (F: 5' AAGACGATCAGATACCGTCGTAG 3'; R: 5' GTTTCAGCTTTGC AACCACTACTC 3') or β actin abundance. Real time PCR primer sequences are as follows: mouse EglN2 (F: 5' CTGGGCAACTACGTCATCAAT 3'; R: 5' TG CACCTTAACATCCCAGTTC 3'); mouse Cyclin D1 (F: CCAACAACCTCCTC TCCTGCT 3'; R: 5' GACTCCAGAAGGGCTTCAATC 3'); mouse β actin (F: 5' ACCAAGTGGACGACATGGA 3'; R: 5' GGTCTCAAACATGATCTGGGTC AT 3'); human EglN2 (F: 5' AACATCGAGCCACTCTTTGAC 3'; R: 5' TCCTT GGCATCAAATACCAG 3'); human Cyclin D1 (F: 5' CCGTCCATGCGGAAG ATC 3'; R: 5' ATGGCCAGCGGAAGAC 3'); human β actin (F: 5' AGAAAA TCTGGCACCACACC 3'; R: 5' GGGGTGTTGAAGGTCTCAA 3').

Plasmids

The EglN2 open reading frame cDNA was PCR amplified with a 5' primer that introduced a BamHI site and a Flag epitope and a 3' primer that introduced an EcoRI site. The product was digested with BamHI and EcoRI and cloned into pBabe Puro vector cut with these two enzymes. pBABE EglN2 H358A was made using a site directed mutagenesis kit (Quick change; Stratagene). pBabeHygro Cyclin D1 was constructed by ligating the BamHI Sall Cyclin D1 cDNA insert from pBabePuro Cyclin D1 (provided by P. Sicinski) into pBabeHygro vector cut with these two enzymes. pLXSN and pLXSN E7 retroviral vectors (Halbert et al., 1991) were given by K. Munger.

shRNA expression vectors corresponding to the siRNAs described above were created by ligating synthetic, duplex oligonucleotides into pMKO.1 retroviral vector (Boehm et al., 2005) or pCCLsin.PPT.hPGK.GFP.Wpre lentiviral vector (Corso et al., 2008) (provided by S. Giordano). All plasmids were confirmed by DNA sequencing.

Lentiviral Rb shRNA vectors, ARNT shRNA vectors, and lentiviral EglN2 shRNA (TRC00000324 328) were obtained from the Broad Institute TRC shRNA library. Rb #1 shRNA target sequence: 5' CCACATTATTCTAGTCCA AA 3'; Rb #2 shRNA target sequence: 5' CAGAGATCGTGTATTGAGATT 3'; ARNT target sequences: 5' CCTTTGTCTTTCTGTGTAATT 3' (Figure 1) and 5' GAGAAGTCAGATGGTTTATTT 3' (Figure S5); TRC00000324 328 shRNA target sequences: 5' CGCATGGCAGACAGCTTAAAT 3'; 5' GCTGCATCACC TGATATCTATT 3'; 5' GCCACTCTTTGACCGGTTGCT 3'; 5' ACTGGGACGTTA AGGTGCATG 3'; 5' CTGGGACGTTAAGGTGCATGG 3', respectively. The lentivirus encoding the HIF2 α was a gift of S. Lee.

Virus Production and Infection

Phoenix packaging cell line was used for the generation of ecotropic retroviruses and all retroviral infections were carried out as described previously (Boehm et al., 2005). 293T packaging cell line was used for lentiviral amplification and all lentiviral infections were carried out as previously described (Moffat et al., 2006). In brief, viruses were collected 48 and 72 hr after transfection, filtered, and used for infecting cells in the presence of 8 $\mu\text{g/ml}$ polybrene prior to drug selection.

Microarray Analysis

The gene expression data set (www.ncbi.nlm.nih.gov/geo/; accession number GSE5460) and immunohistochemical analysis of primary human breast tumors used for Figure 3D was done as described in Lu et al. (2008). Raw expression data obtained with Affymetrix GENECHIP software was normalized, analyzed, and displayed with DNA Chip Analyzer (dChip) custom software (<http://www.dChip.org/>). Array probe data were normalized to the mean expression level of

each probe across the sample set. The analysis in Figure 3C and Figure S4 was performed with data and software available at <http://www.oncomine.org> and <http://www.genesapiens.org>, respectively.

For Figure S10 and Tables S1 S3, T47D breast carcinoma cells that were infected with lentivirus encoding either inducible EglN2 shRNA or Scrambled control (Scr) shRNA were treated with doxycycline (1 $\mu\text{g/ml}$) for 48 hr or left untreated. Total RNA was extracted by using RNeasy mini kit with on column DNase digestion (QIAGEN). Biotin labeled cRNA was prepared from 1 μg of total RNA, fragmented, and hybridized to a Human Gene 1.0ST array (Affymetrix). The arrays were scanned and the data, as CEL files, were analyzed with Affymetrix Expression Console. The data were normalized using RMA (Robust Multi Array) normalization (Bolstad et al., 2003). All samples successfully underwent a series of quality control tests and results from duplicate samples were highly comparable ($R > 0.967$). Gene expression values less than a minimum threshold of 20 or a maximum threshold of 16,000 were set to 20 and 16,000, respectively. Genes with minimal variation across the data set were discarded (maximum/minimum < 3 or maximum minimum < 100). GSEA was performed as described previously (Subramanian et al., 2005).

Cell Proliferation Assays

T47D, BT 474, and ZR 75 1 cells were plated, in triplicate, in 6 well plates (10^5 cells/well) in RPMI supplemented with 10% FBS or in phenol red free RPMI containing 5% charcoal stripped serum supplemented, as indicated, with 10 nM estrogen. At the indicated time points, cells were trypsinized, pelleted by centrifugation, and resuspended in RPMI supplemented with 0.2% Trypan blue. The number of viable cells, as determined by Trypan blue exclusion, was determined with a hemocytometer.

shRNA Pooled Screening

Pooled RNAi screens consisting of 45,000 shRNAs were conducted as described by Luo et al. (2008). In brief, an shRNA pool consisting of 45,182 individual constructs was infected into the indicated cancer cell lines. For each screen, 3.6×10^7 cells were infected at a multiplicity of infection of 0.3 for ensuring that each shRNA was introduced into 200 independent cells. Early time point (3 4 day) samples ($n = 10$) and DNA control samples ($n = 10$) were compared with end time point (4 weeks) samples derived from replicate ($n = 10$) infections of each cell line. Genomic DNA was prepared from these time points and the hairpin region of shRNA constructs was amplified and digested to create half hairpin barcodes that were hybridized to a custom Affymetrix microarray. After microarray normalization, fold depletion scores for EglN2 were calculated on a construct by construct basis by comparing late time point hybridization values to early time point hybridization values.

RIGER Algorithm

RNAi gene enrichment ranking (RIGER), a statistical approach that considers the phenotypic results for the multiple shRNA constructs targeting the same gene, was deployed as described (Luo et al., 2008). Briefly, this approach is based on the GSEA methodology (Subramanian et al., 2005) and uses similar Kolmogorov Smirnov based statistics to calculate gene scores from a data set of shRNA construct profiles. First, shRNA constructs targeting EglN2 were scored according to their differential effects between late and early time points for each cell line. An Enrichment Score was calculated for each cell line, indicating the enrichment or depletion for the five EglN2 hairpins treated as a set. Finally, to find genes frequently essential across multiple cell lines, a second application of RIGER was used to find genes for which the hairpins targeting the gene were depleted in at least 8/12 cell lines.

Orthotopic Tumor Growth Assays

Six week old female nude mice (Taconic) were used for xenograft studies. Approximately 8×10^6 viable tumor cells were resuspended in 40 μl growth factor reduced Matrigel (BD Biosciences) and injected orthotopically into mammary gland four as previously described (Minn et al., 2005). Mice were supplied with chow containing 6 g doxycycline/kg (Bioserv) for a treatment period of 5 6 weeks.

For bioluminescent detection and quantification of cancer cells, mice were given a single i.p. injection of a mixture of luciferin (50 mg/kg), ketamine (150 mg/kg), and xylazine (12 mg/kg) in sterile water. Five minutes later, mice were placed in a light tight chamber equipped with a charge coupled

device IVIS imaging camera (Xenogen). Photons were collected for a period of 1 60 s, and images were obtained by using LIVING IMAGE 2.60.1 software (Xenogen) and quantified using IGOR Pro 4.09A image analysis software (WaveMetrics). The total photons from the EglN2 shRNA tumor region of interest (ROI) were divided by the total photons from Scrambled shRNA tumor ROI and, for each mouse, normalized based on the ratio prior to the onset of doxycycline treatment for that mouse. Results were presented as mean \pm standard error of the mean (SEM).

ACCESSION NUMBERS

Microarray data from T47D cells harvested 0 or 48 hr after induction of an shRNA against EglN2 or a scrambled control shRNA were deposited in the NIH Gene Expression Omnibus database (accession number GSE18171).

SUPPLEMENTAL DATA

Supplemental Data include 13 figures, Supplemental Experimental Procedures, and three tables and can be found with this article online at [http://www.cell.com/cancer-cell/supplemental/S1535-6108\(09\)00343-2](http://www.cell.com/cancer-cell/supplemental/S1535-6108(09)00343-2).

ACKNOWLEDGMENTS

We thank Regeneron Pharmaceuticals for the *EglN2*^{-/-} mice, Oliver Hankinson for the *ARNT*^{-/-} cells, Silvia Giordano for the inducible shRNA vector, Yan Geng for help with mammary gland analysis, Margaret McLaughlin Drubin for help with E7 immunoblots, Mariela Jaskelioff for help with xenograft studies, and members of the Kaelin Laboratory for useful discussions. This work was supported by National Cancer Institute Dana Farber/Harvard SPORE in Breast Cancer (A.L.R.) and the Breast Cancer Research Foundation (A.L.R. and W.G.K.). Q.Z. is supported by a postdoctoral fellowship from Terri Brodeur Breast Cancer Foundation. W.G.K. is a Howard Hughes Medical Institute Investigator and a Doris Duke Distinguished Clinical Investigator. This work is supported in part by a National Institutes of Health grant (5R01CA068490-14) to W.G.K. W.G.K. owns equity in Fibrogen, Inc., which is developing prolyl hydroxylase inhibitors as potential therapeutics.

Received: May 18, 2009

Revised: September 11, 2009

Accepted: September 25, 2009

Published: November 2, 2009

REFERENCES

Appelhoff, R.J., Tian, Y.M., Raval, R.R., Turley, H., Harris, A.L., Pugh, C.W., Ratcliffe, P.J., and Gleadle, J.M. (2004). Differential function of the prolyl hydroxylases PHD1, PHD2, and PHD3 in the regulation of hypoxia inducible factor. *J. Biol. Chem.* *279*, 38458–38465.

Aragones, J., Schneider, M., Van Geyte, K., Fraisl, P., Dresselaers, T., Mazzone, M., Dirx, R., Zacchigna, S., Lemieux, H., Jeoung, N.H., et al. (2008). Deficiency or inhibition of oxygen sensor Phd1 induces hypoxia tolerance by reprogramming basal metabolism. *Nat. Genet.* *40*, 170–180.

Aravind, L., and Koonin, E.V. (2001). The DNA repair protein AlkB, EGL 9, and leprecan define new families of 2-oxoglutarate and iron dependent dioxygenases. *Genome Biol.* *2*, research0007.

Bartkova, J., Lukas, J., Muller, H., Luthjohann, D., Strauss, M., and Bartek, J. (1994). Cyclin D1 protein expression and function in human breast cancer. *Int. J. Cancer* *57*, 353–361.

Berra, E., Benizri, E., Ginouves, A., Volmat, V., Roux, D., and Pouyssegur, J. (2003). HIF prolyl hydroxylase 2 is the key oxygen sensor setting low steady state levels of HIF 1alpha in normoxia. *EMBO J.* *22*, 4082–4090.

Boehm, J.S., Hession, M.T., Bulmer, S.E., and Hahn, W.C. (2005). Transformation of human and murine fibroblasts without viral oncoproteins. *Mol. Cell. Biol.* *25*, 6464–6474.

Bolstad, B.M., Irizarry, R.A., Astrand, M., and Speed, T.P. (2003). A comparison of normalization methods for high density oligonucleotide array data based on variance and bias. *Bioinformatics* *19*, 185–193.

Boyer, S.N., Wazer, D.E., and Band, V. (1996). E7 protein of human papilloma virus 16 induces degradation of retinoblastoma protein through the ubiquitin proteasome pathway. *Cancer Res.* *56*, 4620–4624.

Bruegge, K., Jelkmann, W., and Metzner, E. (2007). Hydroxylation of hypoxia inducible transcription factors and chemical compounds targeting the HIF alpha hydroxylases. *Curr. Med. Chem.* *14*, 1853–1862.

Brugarolas, J., Lei, K., Hurley, R.L., Manning, B.D., Relling, J.H., Hafen, E., Witters, L.A., Ellisen, L.W., and Kaelin, W.G., Jr. (2004). Regulation of mTOR function in response to hypoxia by REDD1 and the TSC1/TSC2 tumor suppressor complex. *Genes Dev.* *18*, 2893–2904.

Corso, S., Migliore, C., Ghiso, E., De Rosa, G., Comoglio, P.M., and Giordano, S. (2008). Silencing the MET oncogene leads to regression of experimental tumors and metastases. *Oncogene* *27*, 684–693.

Epstein, A.C., Gleadle, J.M., McNeill, L.A., Hewitson, K.S., O'Rourke, J., Mole, D.R., Mukherji, M., Metzner, E., Wilson, M.I., Dhanda, A., et al. (2001). C. elegans EGL 9 and mammalian homologs define a family of dioxygenases that regulate HIF by prolyl hydroxylation. *Cell* *107*, 43–54.

Frei, C., and Edgar, B.A. (2004). Drosophila cyclin D/Cdk4 requires Hif 1 prolyl hydroxylase to drive cell growth. *Dev. Cell* *6*, 241–251.

Geng, Y., Whoriskey, W., Park, M.Y., Bronson, R.T., Medema, R.H., Li, T., Weinberg, R.A., and Sicinski, P. (1999). Rescue of cyclin D1 deficiency by knockin cyclin E. *Cell* *97*, 767–777.

Halbert, C.L., Demers, G.W., and Galloway, D.A. (1991). The E7 gene of human papillomavirus type 16 is sufficient for immortalization of human epithelial cells. *J. Virol.* *65*, 473–478.

Hsieh, M.M., Linde, N.S., Wynter, A., Metzger, M., Wong, C., Langsetmo, I., Lin, A., Smith, R., Rodgers, G.P., Donahue, R.E., et al. (2007). HIF prolyl hydroxylase inhibition results in endogenous erythropoietin induction, erythrocytosis, and fetal hemoglobin expression in rhesus macaques. *Blood* *110*, 2140–2147.

Kaelin, W.G., Jr., and Ratcliffe, P.J. (2008). Oxygen sensing by metazoans: The central role of the HIF hydroxylase pathway. *Mol. Cell* *30*, 393–402.

Klose, R.J., Kallin, E.M., and Zhang, Y. (2006). JmjC domain containing proteins and histone demethylation. *Nat. Rev. Genet.* *7*, 715–727.

Kozar, K., Ciemerych, M.A., Rebel, V.I., Shigematsu, H., Zagozdzon, A., Sicinska, E., Geng, Y., Yu, Q., Bhattacharya, S., Bronson, R.T., et al. (2004). Mouse development and cell proliferation in the absence of D cyclins. *Cell* *118*, 477–491.

Landis, M.W., Pawlyk, B.S., Li, T., Sicinski, P., and Hinds, P.W. (2006). Cyclin D1 dependent kinase activity in murine development and mammary tumorigenesis. *Cancer Cell* *9*, 13–22.

Laughner, E., Taghavi, P., Chiles, K., Mahon, P.C., and Semenza, G.L. (2001). HER2 (neu) signaling increases the rate of hypoxia inducible factor 1alpha (HIF 1alpha) synthesis: Novel mechanism for HIF 1 mediated vascular endothelial growth factor expression. *Mol. Cell. Biol.* *21*, 3995–4004.

Li, Y.M., Zhou, B.P., Deng, J., Pan, Y., Hay, N., and Hung, M.C. (2005). A hypoxia independent hypoxia inducible factor 1 activation pathway induced by phosphatidylinositol 3 kinase/Akt in HER2 overexpressing cells. *Cancer Res.* *65*, 3257–3263.

Lu, X., Lu, X., Wang, Z.C., Iglehart, J.D., Zhang, X., and Richardson, A.L. (2008). Predicting features of breast cancer with gene expression patterns. *Breast Cancer Res. Treat.* *108*, 191–201.

Luo, B., Cheung, H.W., Subramanian, A., Sharifnia, T., Okamoto, M., Yang, X., Hinkle, G., Boehm, J.S., Beroukhi, R., Weir, B.A., et al. (2008). Highly parallel identification of essential genes in cancer cells. *Proc. Natl. Acad. Sci. USA* *105*, 20380–20385.

Maxwell, P.H., Wiesener, M.S., Chang, G. W., Clifford, S.C., Vaux, E.C., Cockman, M.E., Wykoff, C.C., Pugh, C.W., Maher, E.R., and Ratcliffe, P.J. (1999). The tumour suppressor protein VHL targets hypoxia inducible factors for oxygen dependent proteolysis. *Nature* *399*, 271–275.

- Metzen, E., Berchner-Pfannschmidt, U., Stengel, P., Marxsen, J.H., Stolze, I., Klinger, M., Huang, W.Q., Wotzlaw, C., Hellwig-Burgel, T., Jelkmann, W., et al. (2003). Intracellular localisation of human HIF-1 alpha hydroxylases: Implications for oxygen sensing. *J. Cell Sci.* *116*, 1319–1326.
- Minamishima, Y.A., Moslehi, J., Bardeesy, N., Cullen, D., Bronson, R.T., and Kaelin, W.G., Jr. (2008). Somatic inactivation of the PHD2 prolyl hydroxylase causes polycythemia and congestive heart failure. *Blood* *111*, 3236–3244.
- Minamishima, Y.A., Moslehi, J., Padera, R.F., Bronson, R.T., Liao, R., and Kaelin, W.G., Jr. (2009). A feedback loop involving the Phd3 prolyl hydroxylase tunes the mammalian hypoxic response in vivo. *Mol. Cell Biol.*, in press. Published online August 31, 2009. MCB.00331-09v1.
- Minn, A.J., Gupta, G.P., Siegel, P.M., Bos, P.D., Shu, W., Giri, D.D., Viale, A., Olshen, A.B., Gerald, W.L., and Massague, J. (2005). Genes that mediate breast cancer metastasis to lung. *Nature* *436*, 518–524.
- Moffat, J., Grueneberg, D.A., Yang, X., Kim, S.Y., Kloepfer, A.M., Hinkle, G., Piqani, B., Eisenhaure, T.M., Luo, B., Grenier, J.K., et al. (2006). A lentiviral RNAi library for human and mouse genes applied to an arrayed viral high-content screen. *Cell* *124*, 1283–1298.
- Mole, D.R., Schlemminger, I., McNeill, L.A., Hewitson, K.S., Pugh, C.W., Ratcliffe, P.J., and Schofield, C.J. (2003). 2-oxoglutarate analogue inhibitors of HIF prolyl hydroxylase. *Bioorg. Med. Chem. Lett.* *13*, 2677–2680.
- Nakayama, K., Frew, I.J., Hagensen, M., Skals, M., Habelhah, H., Bhoumik, A., Kadoya, T., Erdjument-Bromage, H., Tempst, P., Frappell, P.B., et al. (2004). Siah2 regulates stability of prolyl-hydroxylases, controls HIF1alpha abundance, and modulates physiological responses to hypoxia. *Cell* *117*, 941–952.
- Neuman, E., Ladha, M.H., Lin, N., Upton, T.M., Miller, S.J., DiRenzo, J., Pestell, R.G., Hinds, P.W., Dowdy, S.F., Brown, M., and Ewen, M.E. (1997). Cyclin D1 stimulation of estrogen receptor transcriptional activity independent of cdk4. *Mol. Cell Biol.* *17*, 5338–5347.
- Ozer, A., and Bruick, R.K. (2007). Non-heme dioxygenases: Cellular sensors and regulators jelly rolled into one? *Nat. Chem. Biol.* *3*, 144–153.
- Pollard, P.J., Loenarz, C., Mole, D.R., McDonough, M.A., Gleadle, J.M., Schofield, C.J., and Ratcliffe, P.J. (2008). Regulation of Jumonji-domain-containing histone demethylases by hypoxia-inducible factor (HIF)-1alpha. *Biochem. J.* *416*, 387–394.
- Rantanen, K., Pursiheimo, J., Hogel, H., Himanen, V., Metzen, E., and Jaakkola, P.M. (2008). Prolyl hydroxylase PHD3 activates oxygen-dependent protein aggregation. *Mol. Biol. Cell* *19*, 2231–2240.
- Reiling, J.H., and Hafen, E. (2004). The hypoxia-induced paralogs Scylla and Charybdis inhibit growth by down-regulating S6K activity upstream of TSC in *Drosophila*. *Genes Dev.* *18*, 2879–2892.
- Roy, P.G., and Thompson, A.M. (2006). Cyclin D1 and breast cancer. *Breast* *15*, 718–727.
- Safran, M., Kim, W.Y., O'Connell, F., Flippin, L., Gunzler, V., Horner, J.W., Depinho, R.A., and Kaelin, W.G., Jr. (2006). Mouse model for noninvasive imaging of HIF prolyl hydroxylase activity: Assessment of an oral agent that stimulates erythropoietin production. *Proc. Natl. Acad. Sci. USA* *103*, 105–110.
- Schlisio, S., Kenchappa, R.S., Vredevelde, L.C., George, R.E., Stewart, R., Greulich, H., Shahriari, K., Nguyen, N.V., Pigny, P., Dahia, P.L., et al. (2008). The kinesin KIF1Bbeta acts downstream from EglN3 to induce apoptosis and is a potential p36 tumor suppressor. *Genes Dev.* *22*, 884–893.
- Semenza, G.L. (2003). Targeting HIF-1 for cancer therapy. *Nat. Rev. Cancer* *3*, 721–732.
- Seth, P., Krop, I., Porter, D., and Polyak, K. (2002). Novel estrogen and tamoxifen induced genes identified by SAGE (Serial Analysis of Gene Expression). *Oncogene* *21*, 836–843.
- Sicinski, P., Donaher, J.L., Parker, S.B., Li, T., Fazeli, A., Gardner, H., Haslam, S.Z., Bronson, R.T., Elledge, S.J., and Weinberg, R.A. (1995). Cyclin D1 provides a link between development and oncogenesis in the retina and breast. *Cell* *82*, 621–630.
- Steeg, P.S., and Zhou, Q. (1998). Cyclins and breast cancer. *Breast Cancer Res. Treat.* *52*, 17–28.
- Subramanian, A., Tamayo, P., Mootha, V.K., Mukherjee, S., Ebert, B.L., Gillette, M.A., Paulovich, A., Pomeroy, S.L., Golub, T.R., Lander, E.S., and Mesirov, J.P. (2005). Gene set enrichment analysis: A knowledge-based approach for interpreting genome-wide expression profiles. *Proc. Natl. Acad. Sci. USA* *102*, 15545–15550.
- Takeda, K., Ho, V.C., Takeda, H., Duan, L.J., Nagy, A., and Fong, G.H. (2006). Placental but not heart defects are associated with elevated hypoxia-inducible factor alpha levels in mice lacking prolyl hydroxylase domain protein 2. *Mol. Cell Biol.* *26*, 8336–8346.
- Takeda, K., Aguila, H.L., Parikh, N.S., Li, X., Lamothe, K., Duan, L.J., Takeda, H., Lee, F.S., and Fong, G.H. (2008). Regulation of adult erythropoiesis by prolyl hydroxylase domain proteins. *Blood* *111*, 3229–3235.
- Taylor, M.S. (2001). Characterization and comparative analysis of the EGLN gene family. *Gene* *275*, 125–132.
- Tian, Y.M., Mole, D.R., Ratcliffe, P.J., and Gleadle, J.M. (2006). Characterization of different isoforms of the HIF prolyl hydroxylase PHD1 generated by alternative initiation. *Biochem. J.* *397*, 179–186.
- Yu, Q., Geng, Y., and Sicinski, P. (2001). Specific protection against breast cancers by cyclin D1 ablation. *Nature* *411*, 1017–1021.
- Yu, Q., Sicinska, E., Geng, Y., Ahnstrom, M., Zagodzón, A., Kong, Y., Gardner, H., Kiyokawa, H., Harris, L.N., Stal, O., and Sicinski, P. (2006). Requirement for CDK4 kinase function in breast cancer. *Cancer Cell* *9*, 23–32.
- Zwijsen, R.M., Wientjens, E., Klompaker, R., van der Sman, J., Bernards, R., and Michalides, R.J. (1997). CDK-independent activation of estrogen receptor by cyclin D1. *Cell* *88*, 405–415.